IOP PUBLISHING JOURNAL OF PHYSICS D: APPLIED PHYSICS

J. Phys. D: Appl. Phys. **41** (2008) 135103 (7pp) doi:10.1088/0022-3727/41/13/135103

Gamma irradiation-induced changes at the electrical characteristics of organic-based Schottky structures

Ö Güllü[1,3], M Çankaya[2], M Biber[1] and A Türüt[1]

[1] Department of Physics, Atatürk University, Erzurum, Turkey
[2] Department of Chemistry, Atatürk University, Erzurum, Turkey

E-mail: omergullu@gmail.com (Ö Güllü)

Received 20 March 2008, in final form 30 April 2008
Published 6 June 2008
Online at stacks.iop.org/JPhysD/41/135103

Abstract

We have studied electrical parameters of an Al/methyl violet/p-Si Schottky device by using current–voltage and capacitance–voltage–frequency measurements under γ irradiation at room temperature. Experimental results have shown that γ radiation gives rise to an increase in the barrier height, the ideality factor and the interfacial state density, while the series resistance decreases by applied radiation.

(Some figures in this article are in colour only in the electronic version)

1. Introduction

Organic films on an inorganic semiconductor modify the electronic properties of metal–semiconductor (MS) contacts. Schottky barrier heights (SBHs) of the MS contacts can be manipulated by the insertion of an organic layer between the semiconductor and the metal film. Campbell *et al* [1] have used organic thin films to introduce a controlled dipole layer at the semiconductor/organic interface and thus change the SBH. They [1] reported that the Schottky barrier could be either increased or decreased by using an organic thin layer on an inorganic semiconductor. They also reported that changes in the SBH were more than 500 meV. In this way, the organic layer based Schottky diodes were superior with respect to conventional Schottky diodes due to modified contact barriers [1]. By means of the choice of the organic molecule and the interlayer thickness, the device can be designed to exhibit the desired properties. Thereby, the inclusion of thin films of organic semiconductors with nanometre thickness in inorganic Schottky diodes introduces a method to control the fundamental device parameters [2–6]. Methyl violet with the molecular formula $C_{25}H_{30}ClN_3$ used in this work is a typical aromatic azo compound. It is an organic dye molecule used extensively as an acid–base indicator due to its radical colour change with varying pH. Its colour originates from absorbance in the visible region of the spectrum due to the delocalization of electrons in the benzene and azo groups forming a conjugated system. The molecular structure of methyl violet is shown in figure 1. The structure of azo dyes has attracted considerable attention recently due to their wide applicability in the light-induced photo isomerization process and their potential usage for reversible optical data storage [7–9].

When any radiation such as gamma radiation as well as electron, neutron, proton and alpha particle with energies in the range of 1 keV to hundreds of MeV passes through the semiconductor device different effects may occur [10, 11]. High energy radiation penetrates into the MS interface and causes damage deep below the interface. Low energy radiation causes severe lattice damage in the form of vacancies, interstitials and defect complexes at the near interface of the device [12–16]. The irradiation-induced electrically active defects act either as traps or as recombination centres in the semiconductors, depending on the capture cross-sections of the electrons and holes [10]. The defects created at the interface via gamma irradiation reduce the semiconductor free carrier density whereas recombination centres introduce generation–recombination current in rectifying devices [13, 17]. Similarly, the defects result in changing the property of the material at the surface or deep into the surface depending upon the energy of irradiation [10, 11].

Knowledge of the influence of radiation damage on the Schottky barrier diodes (SBDs) performance is a

[3] Author to whom any correspondence should be addressed.

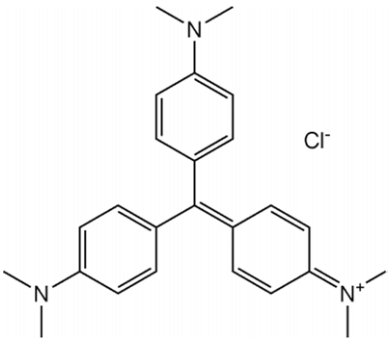

Figure 1. Molecular structure of the methyl violet organic compound.

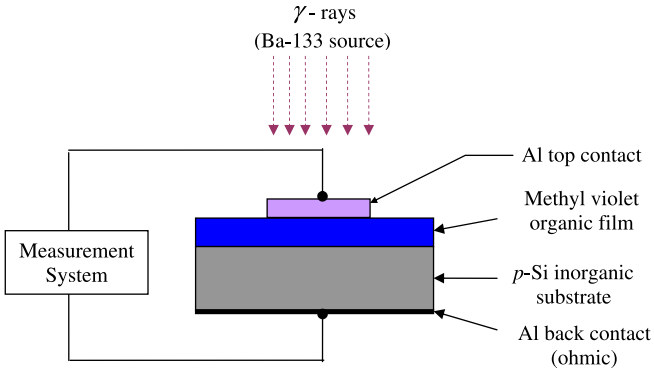

Figure 2. (Colour online) Experimental setup for electrical measurements and the irradiation process of the Al/methyl violet/p-Si Schottky device.

fundamental field of research, having technological relevance for many applications in semiconductor electronic devices [18]. Hence, it is very much essential to evaluate the effect of irradiation and identify the degradation mechanism to understand the failure mechanisms [15]. Recently, several groups have investigated the effect of gamma-ray irradiation dose on the electrical characteristics of metal/semiconductor (MS), metal/insulator/semiconductor (MIS) and metal/oxide/semiconductor (MOS) structures [17–26, 28–34]. Zainninger and Holmes-Siedle [21], Ma [23, 24] and Winokur *et al* [25] were among the pioneers who made systematic observations on the irradiation behaviour of radiation-induced interface traps in metal/interfacial layer (insulator or oxide)/semiconductor (MIS or MOS) devices. In particular, there are two important effects of radiation to be considered: (a) transient effects due to the electron–hole pair generation and (b) the permanent effect due to the bombardment of devices with radiation, causing changes in the crystal lattice. The radiation-generated holes may diffuse in the insulator, but are less mobile than the electrons; many stationary hole traps are also present. Some workers [18, 33, 34] also reported that particle or gamma irradiation induces defects in the band gap which affects the free carrier concentration and leads to an increase and decrease in the barrier height in p-type and n-type semiconductors, respectively.

In this work, we report on the electrical characteristics of the Al/methyl violet/p-Si Schottky contact (SC) irradiated by a Ba-133 source having γ radiation with 356 keV energy for one day at room temperature. After the irradiation process, we present the changes in electrical characteristics evaluated using the current–voltage (I–V) and capacitance–voltage–frequency (C–V–f) measurements.

2. Experimental details

2.1. Chemical cleaning and ohmic contact formation

The device was prepared using a one side polished (as received from the manufacturer) p-Si wafer with (1 0 0) orientation and 1×10^{15} cm^{-3} doping density. The wafer was chemically cleaned using the RCA cleaning procedure (i.e. 10 min boiling in $NH_3 + H_2O_2 + 6H_2O$ followed by 10 min boiling in $HCl + H_2O_2 + 6H_2O$). The native oxide on the front surface of the substrate was removed in $HF : H_2O$ (1 : 10) solution and was finally rinsed in de-ionized water for 30 s. Then, a low resistivity ohmic back contact to the p-type Si substrate was made by using Al metal, followed by a temperature treatment at 570 °C for 3 min in N_2 atmosphere. The thickness of the Al film was 1200 ± 200 Å.

2.2. Deposition of methyl violet and top contact metallization

A methyl violet organic film was directly formed by adding 10 μL methyl violet solution in methanol (a concentration of 0.2%) on the front surface of the p-Si wafer and by allowing the solvent to dry in N_2 atmosphere. Here, we selected 10 μL of methyl violet solution by considering and testing various factors that could affect the given organic film thickness and homogeneity depending on the solution concentration and the substrate area. The quality of organic thin films should also be related to other factors, such as the film-forming ability, the molecular symmetry and structure [35, 36]. The thickness of the methyl violet film on the Si semiconductor was calculated to be 250 nm from the C–V technique ($C = \varepsilon_s A/d$). Contacting top metal dots with a diameter of 1.0 mm were formed by evaporation of Al. The thickness of the Al film was 1000 ± 200 Å. All evaporation processes were carried out in a vacuum coating unit at about 10^{-5} Torr.

2.3. Electrical and optical measurements

γ radiation with an energy of 356 keV from a Ba-133 source with radioactivity of 10 mCi was used for irradiation of the Al/methyl violet/p-Si contact. The device was irradiated from the top (Schottky metal) metal side for one day at room temperature and in the dark as seen in figure 2. During the irradiation process no bias voltage was applied to the device. The I–V and C–V–f measurements of the device were carried out with a Keithley 487 Picoammeter/Voltage Source and an HP model 4192A LF impedance analyzer at room temperature under dark conditions, respectively. In addition, we wore protective clothes against radiation and used a Pb block for radiation shielding during the electrical measurements. An optical absorbance spectrum of the methyl violet organic film on a glass substrate was obtained with

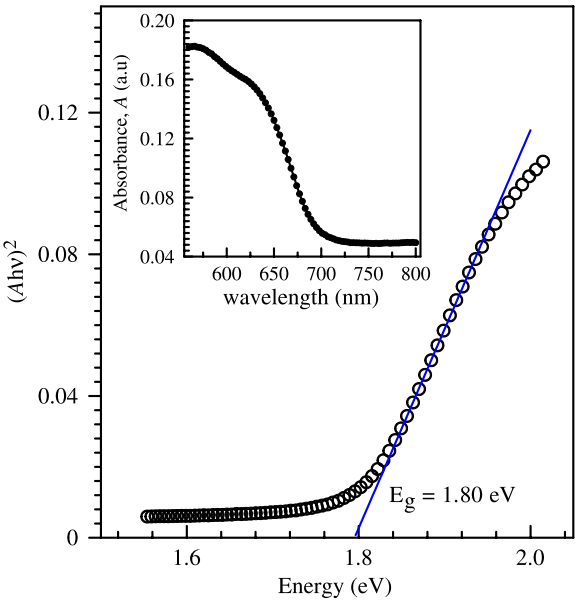

Figure 3. (Colour online) The $(Ah\nu)^2$ versus $h\nu$ plot of the methyl violet organic thin film (the inset shows the optical absorbance spectrum of the methyl violet organic film on a glass substrate).

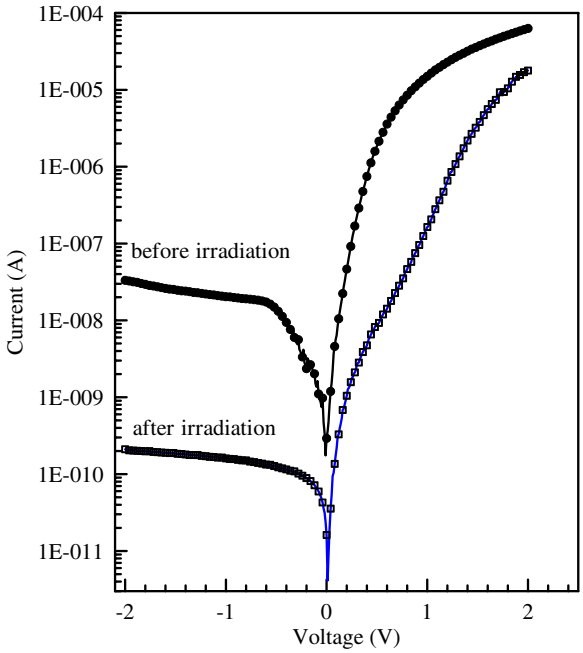

Figure 4. (Colour online) The I–V characteristics of the Al/methyl violet/p-Si Schottky device before and after irradiation.

a spectrophotometer (CHEBIOS-OPTIMUM-ONE UV-VIS spectrophotometer with 190–1100 nm range).

3. Results and discussion

3.1. Optical properties of the methyl violet organic film

The optical absorbance (A) spectrum of the methyl violet organic film was analysed by the following relationship,

$$A(h\nu) = B(h\nu - E_g)^m, \tag{1}$$

where B is a constant and E_g is the optical band gap of the material [37].The exponent m depends on the nature of the transition $m = 1/2, 2, 3/2$ or 3 for allowed direct, allowed non-direct, forbidden direct or forbidden non-direct transitions, respectively. In the inset of figure 3 the graph indicates the optical absorbance spectrum of the methyl violet. Figure 3 shows the plot of $(Ah\nu)^2$ versus $h\nu$ according to equation (1). The optical energy gap E_g of the methyl violet was determined as 1.80 eV by extrapolating the linear portion of this plot at $(Ah\nu)^2 = 0$ for $m = 1/2$, which indicates that the direct transition dominates in the films.

3.2. Electrical properties of the Al/methyl violet/p-Si device

The current through a SBD under a bias voltage is given by the relation [38, 39]

$$I = I_0 \exp\left[\frac{qV}{nkT} - 1\right], \tag{2}$$

where I_0 is the reverse saturation current given by

$$I_0 = AA^{**}T^2 \exp\left(-\frac{q\Phi_b}{kT}\right). \tag{3}$$

Here A is the diode area, $A^{**} = 32\,\mathrm{A\,cm^{-2}\,K^{-2}}$ is the Richardson constant, T is the temperature, k is the Boltzmann constant, q is the electronic charge, Φ_b is the barrier height and n is the ideality factor.

From equations (2) and (3) for $V > 3kT/q$, the ideality factor n and barrier height Φ_b can be written as, respectively:

$$n = \frac{q}{kT}\frac{\mathrm{d}V}{\mathrm{d}\ln(I)} \tag{4}$$

and

$$\Phi_b = \frac{kT}{q}\ln\left(\frac{AA^{**}T^2}{I_0}\right). \tag{5}$$

From the slope of the ln I versus V curve by using equation (4), the value of the ideality factor is calculated. I_0 is determined from the intercept of the ln I versus V curve on the y-axis. Putting the value of I_0 in equation (5), Φ_b can be calculated.

Figure 4 shows room-temperature semi-log I–V characteristics of the Al/methyl violet/p-Si SC device for the cases of before (as-deposited) and after (irradiated) irradiation. The ln I–V curves showed a significant difference after the irradiation process. It was observed that the forward bias current–voltage curves of the device exposed to γ irradiation shifted towards the high voltage side in comparison with the ones before irradiation. As seen from figure 4, both the reverse and forward bias current were also significantly decreased after irradiation. This radiation-induced change observed in both the reverse and forward bias current could be ascribed to the increase in the interfacial defect density [29,40]. This is widely discussed in the following. The values of the ideality factor, the barrier height, the reverse saturation current and the series resistance obtained from forward bias I–V characteristics of the device for the cases of before and after irradiation are given in table 1. As seen in table 1, the barrier height of

Table 1. The various electrical parameters obtained from forward I–V characteristics of the Al/methyl violet/p-Si Schottky device before and after irradiation.

	I–V			$\mathrm{d}V/\mathrm{d}\ln I$		$H(I)$–I		*Norde*	
	Φ_b (eV)	n	I_0 (nA)	n	R_s (kΩ)	Φ_b (eV)	R_s (kΩ)	Φ_b (eV)	R_s (kΩ)
Before irradiation	0.79	2.19	1.230	2.45	28.2	0.78	21.8	0.82	124.0
After irradiation	0.84	5.73	0.194	5.96	23.9	0.83	13.9	0.85	2500.0

the Al/methyl violet/p-Si SBD increases from 0.79 to 0.84 eV after the irradiation process. It has been recently shown by some researchers [18, 33, 34] that the irradiation processes on the Schottky structures induce defects in the band gap which affect the free carrier concentration and lead to an increase (or decrease) in the barrier height in p-type (or n-type) semiconductors. Therefore, the increase in the barrier height after gamma irradiation can be correlated with the modification of the concentration of free carriers at the Al/methyl violet/p-Si interface induced by γ irradiation [18]. Additionally, the increase in the value of the barrier height after irradiation can be explained by the reduction in the carrier concentration in the depletion region of the Al/methyl violet/p-Si Schottky diode through the occurrence of traps and recombination centres associated with radiation damage. It can clearly be seen that the ideality factor of the device also increases from 2.19 to 5.73 after irradiation in table 1. Similar trends have already been reported recently for contacts on other MS structures and have been explained by assuming inhomogeneities at the interface [18, 28].

According to Jayavel *et al* [17], the ideality factor increases due to the inhomogeneity of the interface that depends upon gamma irradiation-induced damage. It shows that the current flow mechanism can be due to other mechanisms. The image-force effect, recombination–generation and tunnelling may be other possible mechanisms that could lead to an ideality factor greater than unity [29]. Additionally, the increase in the ideality factor indicates an increase in the defect density at the interface after γ irradiation, and/or the increase in the ideality factor is due to the lateral inhomogeneity of the barrier height [28]. As a result, the results obtained from I–V characteristics of the device before and after irradiation have been attributed to the presence of a very thin oxide layer plus the organic layer between the metal and the semiconductor [28, 41, 42].

In order to get further insights into the conduction mechanism of reverse characteristics through the irradiated contact, we calculated the reverse saturation current of the γ-irradiated diode and the results are given in table 1. Clearly, there is a significant decrease from 1.23×10^{-9} to 1.94×10^{-10} A at the saturation current of the device after irradiation. The decrease in the reverse current after irradiation may be because deep levels can act as recombination centres and often play the role of carrier recombination in the reverse characteristics [18].

As stated above, it is well known that the downward concave curvature of the forward bias current–voltage plots at sufficiently large voltages is caused by the presence of the effect of R_s, apart from the interface states, which are in equilibrium with the semiconductor [43]. The R_s values have been calculated using a method developed by Cheung and Cheung [44]. According to Cheung and Cheung [44], the forward bias I–V characteristics due to the thermionic emission of a Schottky diode with the series resistance can be expressed as

$$I = I_0 \exp\left[\frac{q(V - IR_s)}{nkT}\right], \tag{6}$$

where the IR_s term is the voltage drop across the series resistance of the device. The values of the series resistance can be determined from the following functions using equation (6).

$$\frac{\mathrm{d}V}{\mathrm{d}(\ln I)} = \frac{nkT}{q} + IR_s, \tag{7}$$

$$H(I) = V - \left(\frac{nkT}{q}\right)\ln\left(\frac{I}{AA^*T^2}\right), \tag{8}$$

and $H(I)$ is given as follows:

$$H(I) = n\Phi_b + IR_s. \tag{9}$$

The plot of $\mathrm{d}V/\mathrm{d}(\ln I)$ versus I is linear and gives R_s as the slope and nkT/q as the y-axis intercept from equation (7). Figure 5(a) shows a plot of $\mathrm{d}V/\mathrm{d}(\ln I)$ versus I at room temperature. The values of n and R_s have been calculated as $n = 2.45$ and $R_s = 28.2\,\mathrm{k}\Omega$ for the case of before irradiation and as $n = 5.96$ and $R_s = 23.9\,\mathrm{k}\Omega$ for the case of after irradiation, respectively. It is observed that there is a relative coincidence between the values of n obtained from the forward bias $\ln I$–V plot and those obtained from the $\mathrm{d}V/\mathrm{d}(\ln I) - I$ curves for both cases.

The plot of $H(I)$ versus I in figure 5(b) using equation (9) gives a straight line with the y-axis intercept equal to the barrier height. The slope of this plot also provides the second determination of R_s which can be used to check the consistency of Cheung's approach. The values of the series resistance calculated from equations (7) and (9) for both before and after irradiation are presented in table 1. As seen from table 1, the values of the series resistance obtained from Cheung's function $\mathrm{d}V/\mathrm{d}(\ln I)$ and $H(I)$ decrease strongly with increasing irradiation and are in good agreement with each other [29, 45].

Norde proposed an alternative method to determine the values of the series resistance and the barrier height [46]. The following function has been defined in the modified Norde's method:

$$F(V) = \frac{V}{\gamma} - \frac{kT}{q}\ln\left(\frac{I(V)}{AA^*T^2}\right), \tag{10}$$

where γ is an arbitrary integer (dimensionless) greater than n. $I(V)$ is the current obtained from the I–V curve. Once the

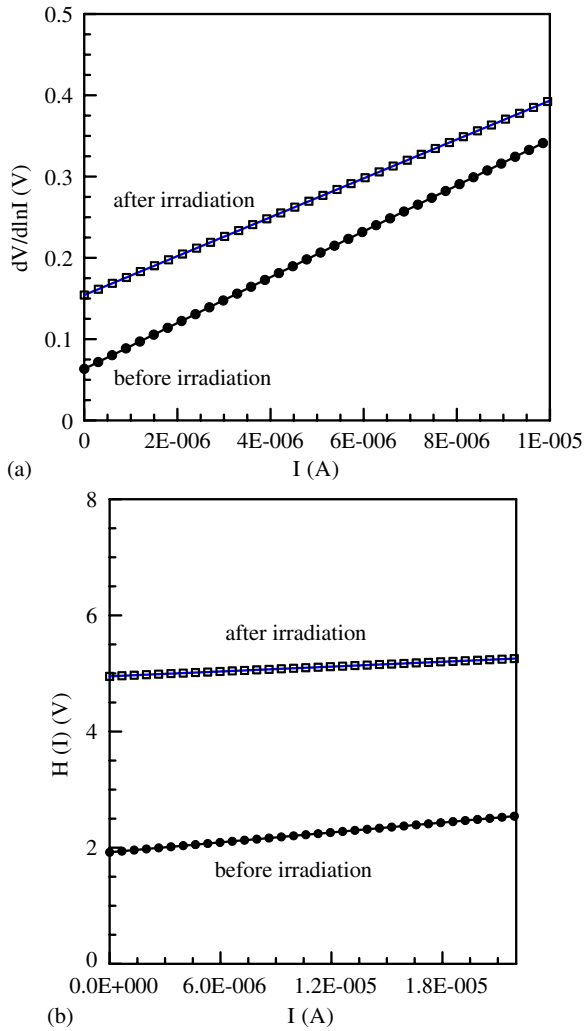

Figure 5. (Colour online) (*a*) dV/d ln I–I and (*b*) $H(I)$–I plots obtained from the experimental I–V of the Al/methyl violet/p-Si device in figure 4 before and after irradiation.

minimum of the F versus V plot is determined, the value of the barrier height can be obtained from equation (11), where $F(V_0)$ is the minimum point of $F(V)$ and V_0 is the corresponding voltage:

$$\Phi_b = F(V_0) + \frac{V_0}{\gamma} - \frac{kT}{q}. \tag{11}$$

Figure 6 shows the $F(V)$–V plot of the junction. From Norde's functions, the R_s value can be determined to be

$$R_s = \frac{kT(\gamma - n)}{qI}. \tag{12}$$

From the F–V plot the values of Φ_b and R_s of the Al/methyl violet/p-Si structure have been determined as 0.82 eV and 124.0 kΩ before irradiation and as 0.85 eV and 2500.0 kΩ after irradiation, respectively. The values of series resistances are dramatically higher than those obtained from the Cheung functions for both cases. Cheung functions are only applied to the nonlinear region in the high voltage region of the forward bias ln I–V characteristics, while Norde's functions are applied to the full forward bias region of the I–V characteristics. Furthermore, the value of the series resistance

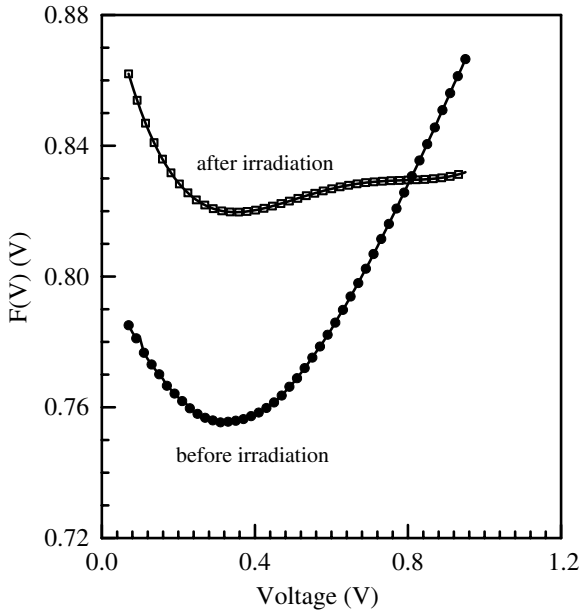

Figure 6. Norde curves obtained from I–V characteristics of the Al/methyl violet/p-Si device before and after irradiation.

may also be very high for the higher ideality factor values. This indicates that the series resistance is a current-limiting factor for this structure. The effect of the series resistance is usually modelled with a series combination of a diode and a resistance R_s. The voltage drop across a diode is expressed in terms of the total voltage drop across the diode and the resistance R_s. The very high series resistance behaviour may be ascribed to the decrease in the exponentially increasing rate in current due to space-charge injection into the methyl violet thin film at a higher forward bias voltage [43]. Thus, Norde's model may not be a suitable method especially for the high ideality factor of the rectifying junctions, which do not agree with pure thermionic emission theory. We assume that another mechanism starts to control the current flow, except for the mechanisms stated above. This mechanism is probably tunnelling, because the tunnelling process is important especially for a thin interfacial layer [43]. However, there is no excellent agreement among the values of Φ_b obtained from the forward bias ln I–V, Cheung functions and Norde functions.

As seen from table 1, the values of the series resistance calculated from Cheung's function [44] decrease for the device after irradiation. The value of the series resistance decreases with the effect of irradiation. Recently, Tataroglu and Altindal [47] demonstrated that the trap charges have enough energy to escape from the traps located between the metal and the semiconductor interface in the Si band gap. Additionally, this decrease for the irradiated device may be attributed to the generation of radiation-induced defect states in energy gap and compensates the free carriers in the substrate [48].

When the interfacial organic film and the natural oxide layer are sufficiently thick, and the transmission probability between the top metal and the interface states is very small, the equation relating N_{ss} and the ideality factor n can be expressed [49] as follows:

$$\frac{1}{n} = \frac{\varepsilon_i}{\varepsilon_i + q^2 N_{ss}\delta}, \tag{13}$$

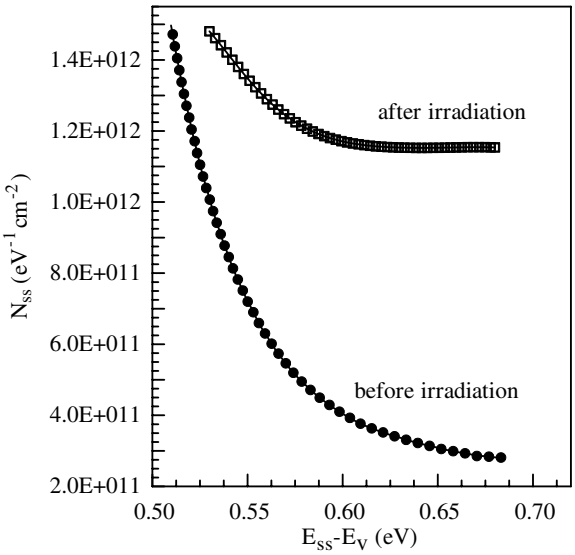

Figure 7. Interface state energy distribution curves of the Al/methyl violet/p-Si Schottky diode both before and after irradiation.

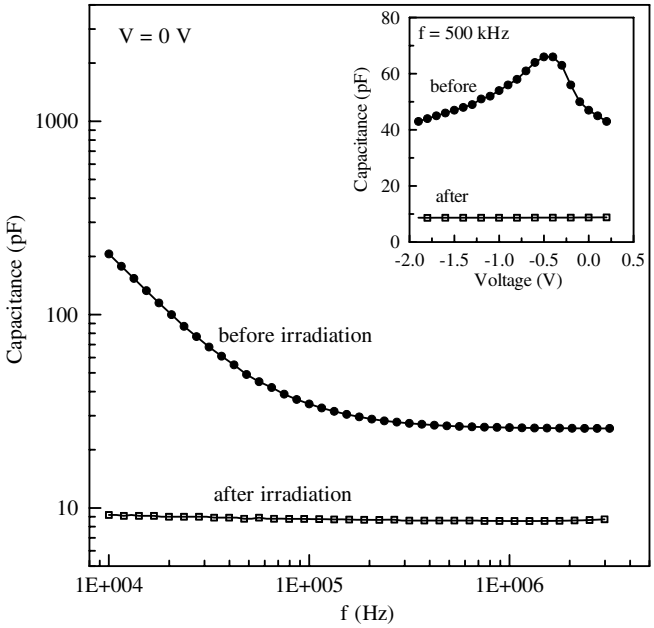

Figure 8. The $C-f$ characteristics of the Al/methyl violet/p-Si Schottky device before and after irradiation (the inset indicates C–V characteristics of the Al/methyl violet/p-Si Schottky device for both cases).

where N_{ss} is the density of the interface states, ε_i the permittivity of the interfacial layer and δ is its thickness. The applied voltage dependence of the barrier height is obtained as

$$\frac{d\Phi_e}{dV} = \beta = 1 - \frac{1}{n(V)}, \tag{14}$$

where β is the voltage coefficient of the effective barrier height Φ_e used in place of the barrier height Φ_b. In the above formulation, for the case that the interface states are in equilibrium with the semiconductor, the bias dependence of the barrier height $d\Phi_e/dV$ is a parameter that combines the effects of both the interface states and the interfacial layer thickness [39, 50]. The effective barrier height is given in the form

$$\Phi_e = \Phi_b + \beta V. \tag{15}$$

In a p-type semiconductor, the energy of the interface states (E_{ss}) with respect to the top of the valance band (E_v) at the surface of the semiconductor is given by

$$E_{ss} - E_v = q\Phi_e - qV. \tag{16}$$

Thus, we can use equations (15) and (16) together with equation (13) in the calculation of the interface state density. By substituting the voltage dependence values of n in equation (13), where $\varepsilon_i = 4\varepsilon_o$, ε_o being the permittivity of free space [39], the values of N_{ss} as a function of V were obtained for both cases. The values of N_{ss} were plotted as a function of $(E_{ss}-E_v)$ by using equation (16). N_{ss} for the Al/methyl violet/p-Si Schottky diode increases exponentially with bias from $2.81 \times 10^{11}\,cm^{-2}\,eV^{-1}$ at $(0.68-E_v)$ eV to $1.50\times10^{12}\,cm^{-2}\,eV^{-1}$ at $(0.51-E_v)$ eV for the case of before irradiation (see figure 7). Also, the interface state density of the Al/methyl violet/p-Si Schottky device after irradiation increases exponentially with bias from $1.15 \times 10^{12}\,cm^{-2}\,eV^{-1}$ at $(0.68 - E_v)$ eV to $1.41 \times 10^{12}\,cm^{-2}\,eV^{-1}$ at $(0.54 - E_v)$ eV (figure 7). This increase in N_{ss} after irradiation is consistent with the above results.

In Schottky diodes, the depletion layer capacitance can be expressed as [38, 39, 51]

$$C = \frac{\varepsilon A}{W} = \sqrt{\frac{q\varepsilon_s N_A A^2}{2\left(V_{bi} - V - \frac{kT}{q}\right)}}, \tag{17}$$

where ε_s is the dielectric constant of the semiconductor, A is the area of the Schottky diode, W is the depletion layer depth, V_{bi} is the built-in potential, N_A is the density of ionized acceptor atoms in the semiconductor and V is the applied reverse bias voltage. The inset of figure 8 shows the C versus V characteristics of the Al/methyl violet/p-Si SC before and after irradiation. As seen from the inset, the capacitance of the device decreases significantly after gamma irradiation. As seen from the inset of figure 8, the capacitance–voltage plot before irradiation has an anomalous peak. This may be attributed to the presence of localized states (interface states which originate from the native oxide layer plus the organic thin layer) at the organic/p-Si interface [27].

Figure 8 also shows the C versus f characteristics of the Al/methyl violet/p-Si Schottky diode before and after irradiation. As seen from both figures, the capacitance of the device decreases significantly after gamma irradiation. According to [20, 28], it may be due to the change in the dielectric constant at the metal/semiconductor interface, and/or according to [20] this may be due to the decrease in the net ionized dopant concentration depending on the irradiation effect. The decrease in the ionized acceptor density with the increase in the irradiation dose is due to generation–recombination through the interface states in the MS interface [28]. According to [28], when the bias injects holes that recombine with the electrons already present in the depletion region, the density of mobile carriers is reduced as a result and the space charge is enhanced further.

4. Conclusion

In conclusion, we have investigated the electrical parameters of the Al/methyl violet/p-Si Schottky diode by using the I–V and C–V–f characteristics under γ irradiation at room temperature. The device was held at a zero bias during gamma irradiation. The basic diode parameters such as ideality factor, barrier height, series resistance and reverse saturation current were extracted from electrical measurements as a function of irradiation. The results indicated that γ irradiation induced an increase in the SBH and the ideality factor. We have also observed that the reverse bias current of the Al/methyl violet/p-Si contact significantly decreased after irradiation. The basic results as related to gamma irradiation have indicated that this device may have applications as radiation sensors in order to detect gamma radiation.

Acknowledgments

The authors wish to thank to C Kaygusuz, Z Elkoca, E Dikicioglu and H Bayrak, Physics Department of Ataturk University, due to their help in experimental measurements.

References

[1] Campbell I H, Rubin S, Zawodzinski T A, Kress J D, Martin R L, Smith D L, Barashkov N N and Ferraris J P 1996 *Phys. Rev.* B **54** 14321
[2] Tada K, Wada M and Onoda M 2003 *J. Phys. D: Appl. Phys.* **36** L70
[3] Roberts A R V and Evans D A 2005 *Appl. Phys. Lett.* **86** 072105
[4] Bolognesi A, Di Carlo A, Lugli P, Kampen T U and Zahn D R T 2003 *J. Phys.: Condens. Matter.* **15** S2719
[5] Kampen T U, Park S and Zahn D R T 2002 *Appl. Surf. Sci.* **190** 461
[6] Cakar M, Temirci C and Turut A 2004 *Synth. Met.* **142** 177
[7] Park S K, Lee C, Min K C and Lee N S 2004 *Bull. Korean Chem. Soc.* **25** 1817
[8] Biswas N and Umapathy S 1997 *J. Phys. Chem.* A **101** 5555
[9] Aydin M E and Turut A 2007 *Microelectron. Eng.* **84** 2875
[10] Jayavel P, Udhayasankar M, Kumar J, Asokan K and Kanjilal D 1999 *Nucl. Instrum. Methods* B **156** 110
[11] Kumar S, Katharria Y S, Kumar S and Kanjilal D 2006 *Solid-State Electron.* **50** 1835
[12] Li S T, Nener B D, Faraone I, Nassibuan A G and Hotchkis M A C 1993 *J. Appl. Phys.* **73** 640
[13] Auret F D, Goodman S A, Erasmus R, Meyer W E and Myburg G 1995 *Nucl. Instrum. Methods* B **106** 323
[14] Arulkumaran S, Arokiaraj J, Dharmarasu N and Kumar J 1996 *Nucl. Instrum. Methods* B **119** 519
[15] Dharmarasu N, Arulkumaran S, Sumathi R R, Jayavel P, Kumar J, Magudapathy P and Nair K G M 1998 *Nucl. Instrum. Methods* B **140** 119
[16] Aliyu Y H, Morgen D V and Bunce R W 1993 *Phys. Status Solidi* a **135** 119
[17] Jayavel P, Kumar J, Santhakumar K, Magudapathy P and Nair K G M 2000 *Vacuum* **57** 51
[18] Mamor M, Sellai A, Bouziane K, Al Harthi S H, Al Busaidi M and Gard F S 2007 *J. Phys. D: Appl. Phys.* **40** 1351
[19] Grove A S and Snow E H 1966 *Proc. IEEE (Lett.)* **54** 894
[20] Singh R, Arora S K and Kanjilal D 2001 *Mater. Sci. Semicond. Process.* **4** 425
[21] Zainninger K H and Holmes-Siedle A G 1967 *RCA Rev.* 208
[22] De Vascancelas E A, Da Silva E F Jr, Khoury H and Freire V N 2000 *Semicond. Sci. Technol.* **15** 794
[23] Ma T P 1989 *Semicond. Sci. Technol.* **4** 1061
[24] Ma T P 1975 *Appl. Phys. Lett.* **27** 615
[25] Winokur P S, McGarrity J M and Boesch H E 1976 *IEEE Trans. Nucl. Sci.* **NS-23** 1580
[26] Tataroglu A, Altindal S, Karadeniz S and Tugluoglu N 2003 *Microelectron. J.* **34** 1043
[27] Jun M, Jang M, Kim Y, Choi C, Kim T, Park B and Lee S 2007 *J. Vac. Sci. Technol.* B **25** 82
[28] Karatas S, Turut A and Altindal S 2005 *Nucl. Instrum. Methods* A **555** 260
Karatas S and Turut A 2006 *Nucl. Instrum. Methods* A **566** 584
[29] Tataroglu A, Altindal S and Bulbul M M 2006 *Nucl. Instrum. Methods* A **568** 863
[30] Coskun C, Gedik N and Balci E 2006 *Semicond. Sci. Technol.* **21** 1656
[31] Tugluoglu N 2007 *Nucl. Instrum. Methods* B **254** 118
[32] Pattabi M, Krishnan S, Ganesh and Mathew X 2007 *Sol. Energy* **81** 111
[33] Fonash S J, Ashok S and Singh R 1981 *Appl. Phys. Lett.* **39** 423
[34] Grussell E, Berg S and Andersson L P 1980 *J. Electrochem. Soc.* **127** 1573
[35] Qiu Y and Qiao J 2000 *Thin Solid Films* **372** 265
[36] Gullu O, Turut A and Asubay S 2008 *J. Phys.: Condens. Matter* **20** 045215
[37] Mott N F and Gurney R W 1940 *Electronic Processes In Ionic Crystals* (London: Oxford University Press)
[38] Sze S M 1981 *Physics of Semiconductor Devices* 2nd edn (New York:Wiley)
[39] Rhoderick E H and Williams R H 1988 *Metal–Semiconductor Contacts* 2nd edn (Oxford: Clarendon)
[40] Gullu O, Demir F, Cimilli F E and Biber M 2008 *Vacuum* **82** 789
[41] Card H C and Rhoderick E H 1971 *J. Phys. D: Appl. Phys.* **4** 1589
[42] Hughes G W 1977 *J. Appl. Phys.* **48** 5357
[43] Gullu O, Aydogan S, Biber M and Turut A 2008 *Vacuum* at press
[44] Cheung S K and Cheung N W 1986 *Appl. Phys. Lett.* **49** 85
[45] Feteha M Y, Soliman M, Gomaa N G and Ashry M 2002 *Renew. Energy* **26** 113
[46] Karatas S, Altindal S, Turut A and Cakar M 2007 *Physica* B **392** 43
[47] Tataroglu A and Altindal S 2006 *Nucl. Instrum. Methods* B **252** 257
[48] Sisodia V, Kabiraj D and Jain I P 2005 *J. Indian Inst. Sci.* **84** 151
[49] Cowley A M and Sze S M 1965 *J. Appl. Phys.* **36** 3212
[50] Tseng H H and Wu C Y 1987 *Solid-State Electron.* **30** 383
[51] Vander Ziel A 1968 *Solid State Physical Electronics* 2nd edn (Englewood Cliffs, NJ: Prentice-Hall)